

## Examination of effectiveness of signal-to-noise ratio factor in estimation of sound speed of medium

媒質の音速推定における信号対雑音比の有効性の検討

Fumitada Sannnou<sup>†</sup>, Ryo Nagaoka<sup>1</sup>, and Hideyuki Hasegawa<sup>1</sup> (<sup>1</sup> Univ. Toyama)

参納史匡<sup>†</sup>, 長岡 亮<sup>1</sup>, 長谷川英之<sup>1</sup> (<sup>1</sup> 富山大院 理工)

### 1. Introduction

Ultrasonic beamforming forms spatially focused directivity to obtain ultrasound images. The delay-and-sum (DAS) beamformer estimates the distance from the scattering point to each ultrasonic transducer and compensates for the time delay of the received signal.

To estimate the time delay, it is necessary to refer to the speed of sound. However, it is difficult to refer to the true speed of sound because the speed of sound varies depending on the tissue type, and the spatial distribution of speeds of sound in the tissue is inhomogeneous.

This research group proposed a method based on the coherence factor (CF) evaluated using echoes from a diffuse scattering medium as an evaluation index [1]. In the present study, signal-to-noise ratio (SNR) factor obtained with linear regression (LR) beamforming is used as another evaluation index.

### 2. Principle

#### 2.1 Beam-forming

In this study, two imaging methods using plane and focused waves are used.

In plane wave imaging, a plane wave was emitted by 96 elements and scattered echoes were received by the same 96 elements. By creating one focused receiving beam with 72 elements, 24 scan lines are obtained in one transmission. By repeating this procedure 4 times, 96 scan lines are obtained.

In focused beam imaging, an ultrasonic beam focused at 20 or 30 mm from the transducer is transmitted. In this study, the number of elements in the transmit aperture was set at 16, 32, 64, and 96. The receive aperture consisted of 96 elements. Consequently, one scan line is obtained with one transmission. By repeating this procedure 121 times, 121 scan lines were formed. **Fig. 1** shows an example of a B-mode image obtained by focused beams.

#### 2.2 Sub-aperture processing

The 96-element receive aperture was divided into sub-apertures, and the outputs from the sub-apertures were used for evaluation of CF and SNR.

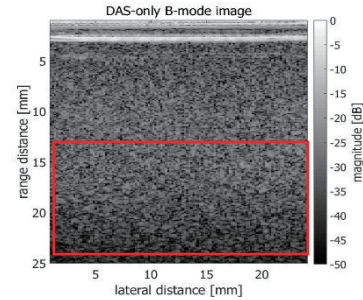


Fig. 1 B-mode image of phantom obtained by focused beams.

### 2.3 Coherence factor

The CF  $CF(m, n)$  at a spatial point  $(m, n)$  in an imaged region is obtained as follows:

$$CF(m, n) = \frac{\left| \frac{1}{K} \sum_{k=0}^{K-1} e_k(m, n) \right|^2}{\frac{1}{K} \sum_{k=0}^{K-1} |e_k(m, n)|^2}, \quad (1)$$

where  $e_k(m, n)$  is the output from the  $k$ -th transducer element or sub-aperture.

### 2.4 SNR factor

The mean squared difference between the measured integrated element signal and its model is calculated as follows:

$$S = \sum (y_i - ax_i - b)^2. \quad (2)$$

The sum of squares  $S$  of the difference between the measured value  $y_i$  and the model  $(ax_i + b)$  is the power of noise. Coefficients  $a$  and  $b$  were determined so as to minimize  $S$ . Finally, SNR factor is calculated as follows:

$$SNR(m, n) = \frac{a^2}{S_{min} + \gamma \cdot a^2}, \quad (3)$$

where  $a^2$  is signal power,  $S_{min}$  is minimized  $S$ , and  $\gamma \cdot a^2$  is added because the denominator diverges to infinity when  $S_{min}$  is 0.

## 3. Method

### 3.1 Estimation of sound speed

The assigned speed of sound was varied from 1480 m/s to 1600 m/s at 5 m/s intervals, and the ultrasound B-mode image, CF, and SNR are estimated. As a result, evaluation indices  $CF_l$  were obtained at 21 different assigned sound speeds. At

each sampled point of  $CF_l$ , the average value  $\overline{CF_l}$  for 21 settings and the maximum value  $CF_{max}$  of  $CF_l$  is calculated.  $\overline{CF_l} / CF_{max}$  at each sampled point is calculated and only the sampled points with values of greater than a threshold value of 0.05 were used. For each of the 21 assigned speeds of sound, the average evaluation indices was obtained from sampled points larger than the threshold, and the speed of sound is estimated from the largest average evaluation index.

### 3.2 Sound speed map

Regions used for evaluation of CF or SNR were 12.24 to 24.48 mm in depth (Region in the red frame in Fig. 1). Furthermore, this region was divided into 10 in the lateral direction and divided into 12 in the depth direction. The sound speed was estimated for each divided area as shown in Fig. 2a. The median filter is applied to the map to obtain a smoothed map as shown in Fig. 2b. The mean estimated sound speed and standard deviation in the area within the red frame were obtained.

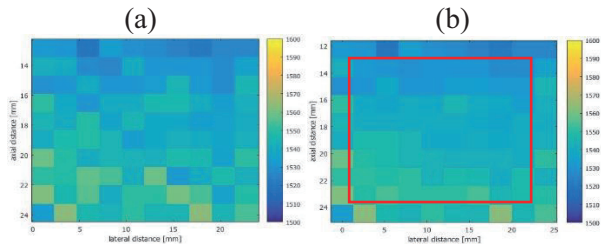


Fig. 2 Map of speed of sound. **a** Before median filter processing. **b** After median filter processing

### 3.3 Experimentation system

In the experiment, a homogeneous scattering medium with a speed of sound of 1540 m/s was used as a phantom. A linear array probe with an element pitch of 0.2 mm and a frequency of 7.5 MHz was used. The sampling frequency was 31.25 MHz.

## 4. Result

As shown in Figs. 3 and 4, the estimation accuracy was improved when using a 20-mm focused wave with an aperture with 16 elements. Also, as shown in Fig. 5a, the estimation accuracy was improved when the CF and SNR factor were obtained with 12 and 24 sub-apertures, respectively. As shown in Fig. 5b when  $\gamma = 0.5$ , the estimation accuracy is further improved using the SNR factor. Fig. 6 shows the estimated map of speeds of sound under the optimum conditions for the CF and SNR. The means and standard deviations of sound speeds estimated from the CF and SNR under those conditions were  $1540.2 \pm 6.3$  m/s and  $1538.7 \pm 3.1$  m/s, respectively.

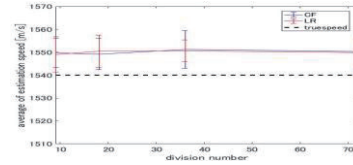


Fig. 3 Means and standard deviations of estimated speeds of sound obtained by changing the number of sub-aperture in plane wave.

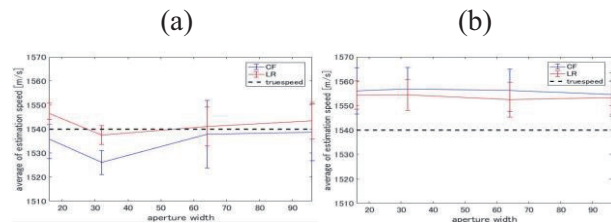


Fig. 4 Means and standard deviations of estimated speeds of sound obtained by changing aperture width. (a) 20-mm focused wave. (b) 30-mm focused wave.

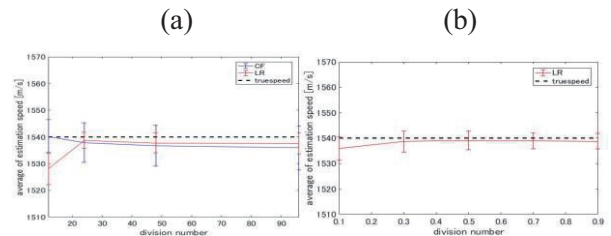


Fig. 5 Means and standard deviations of estimated speeds of sound as functions of (a) the number of sub-aperture and (b)  $\gamma$ .

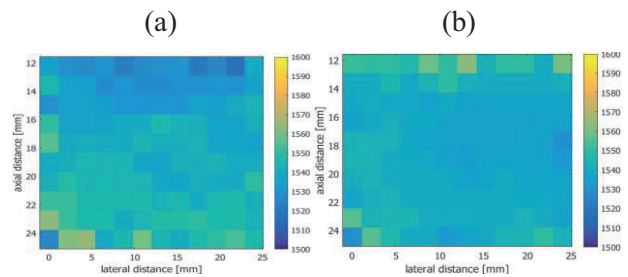


Fig. 6 Maps of estimated speeds of sound obtained under the optimum conditions for (a) CF and (b) SNR.

## 5. Conclusion

In this study, using the evaluation indices, CF and SNR, we investigated the conditions for improving the accuracy of speed of sound estimation by changing the transmit aperture size and the number of sub-apertures. In future work, we plan to use the speed of sound distribution estimated under these optimum conditions to investigate whether the spatial resolution is improved in the beamforming process.

## References

1. H. Hasegawa and R. Nagaoka J. Med. Ultrason. **46** (2019) 297.